

A Conformationally Restricted Gold(III) Complex Elicits Antiproliferative Activity in Cancer Cells

Sailajah Gukathasan, Oluwatosin A. Obisesan, Setareh Saryazdi, Libby Ratliff, Sean Parkin, Robert B. Grossman, and Samuel G. Awuah*



Cite This: <https://doi.org/10.1021/acs.inorgchem.3c02066>



Read Online

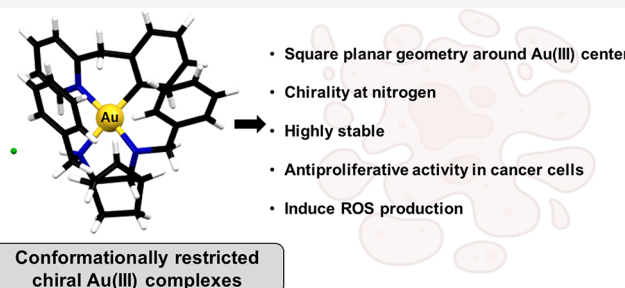
ACCESS |

Metrics & More

Article Recommendations

Supporting Information

ABSTRACT: Diamine ligands are effective structural scaffolds for tuning the reactivity of transition-metal complexes for catalytic, materials, and phosphorescent applications and have been leveraged for biological use. In this work, we report the synthesis and characterization of a novel class of cyclometalated $[\text{C}^{\text{N}}]$ Au(III) complexes bearing secondary diamines including a norbornane backbone, $(2R,3S)$ - N^2,N^3 -dibenzylbicyclo[2.2.1]-heptane-2,3-diamine, or a cyclohexane backbone, $(1R,2R)$ - N^1,N^2 -dibenzylcyclohexane-1,2-diamine. X-ray crystallography confirms the square-planar geometry and chirality at nitrogen. The electronic character of the conformationally restricted norbornane backbone influences the electrochemical behavior with redox potentials of -0.8 to -1.1 V, atypical for Au(III) complexes. These compounds demonstrate promising anticancer activity, particularly, complex **1**, which bears a benzylpyridine organogold framework, and supported by the bicyclic conformationally restricted diaminonorbornane, shows good potency in A2780 cells. We further show that a cellular response to **1** evokes reactive oxygen species (ROS) production and does not induce mitochondrial dysfunction. This class of complexes provides significant stability and reactivity for different applications in protein modification, catalysis, and therapeutics.



INTRODUCTION

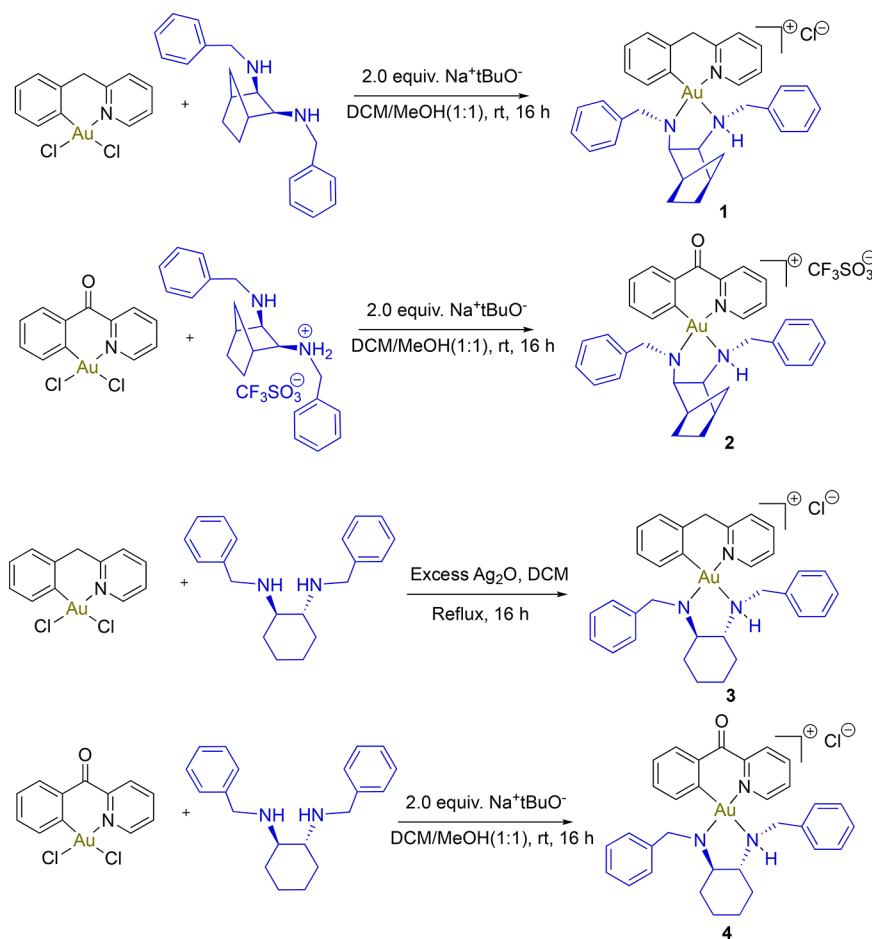
The resurgence of gold (Au) chemistry over the past two decades has contributed to the development of synthetic methods,^{1–4} catalytic transformations,^{5,6} materials for electronics,^{7,8} reagents for bioorthogonal reactions,⁹ protein modifications,^{10,11} and therapeutic agents.^{12–17} In the context of drug discovery, great impetus is derived from auranofin, a Food and Drug Administration (FDA)-approved drug for treating rheumatoid arthritis.¹⁸ Although Au(III) complexes are highly valent and present opportunities for ligand tuning due to having more coordination sites than conventional linear Au(I), the instability of Au(III) has been its Achilles' heel. Ongoing efforts to stabilize the Au(III) center are crucial to accessing complexes for improved performance or activity.^{19–22} Multidentate ligands and cyclometalation to form Au–C bonds are common strategies deployed to resolve this bottleneck associated with Au(III) instability.^{23–30} In addition to the aforementioned strategies, strong σ -donor ligands such as bidentate phosphorus and nitrogen chelates play a dominant role in generating stable Au(III) complexes.^{24,31–34}

There is extensive literature describing the utility of organogold Au(III) complexes in catalysis,^{35–39} materials science,^{40–43} sensors,^{44–46} and anticancer activity.^{47–56} Although organometallic Au(III) complexes bearing N^{N} bidentate ligands with sp^2 -hybridized nitrogen (N) have

recently been reported,^{57–60} bidentate ligands bearing sp^3 -hybridized primary or secondary amines are underexplored, yet they hold tremendous potential for accessing stable but distinct scaffolds.²⁴ This has implications for their reactivity and consequent applications. For example, reports using chiral primary $(1R,2R)$ - $(+)$ -1,2-diaminocyclohexane (DACH) ligands as ancillary ligands of cyclometalated Au(III) give rise to unique structural scaffolds dictated by the starting cyclometalated Au(III) framework.²⁴ It is important to note that chiral Au(III) compounds have garnered immense interest lately, but more is needed in the utility of chiral diamine ligands.^{24,37,61–63} Other water-soluble amine ligands, including biguanide derivatives with good physiological stability and anticancer activity, have also been reported.^{32,64,65} The use of secondary amines as ancillary ligands has the potential to impart metal-center chirality, high stability, and good reactivity for different applications including bioconjugation, medicinal chemistry, catalysis, and materials science.^{66,67}

Received: June 21, 2023

Scheme 1. Synthetic Procedure for Complexes 1–4



In this work, we aimed to prepare stable $[\text{C}^{\text{N}}] \text{Au}(\text{III})$ complexes bearing uncommon N^{NH} chelates derived from chiral secondary amines to generate unprecedented monocationic $[\text{C}^{\text{N}}] \text{Au}^{\text{III}} \text{RN}^{\text{NH}} \text{R}$ derivatives. The secondary diamine ligands used in this work possess a norbornane (bicyclic) backbone or cyclohexane backbone to influence the stability and reactivity due to the conformational constraints imposed by these ligands. The norbornane diamines were synthesized via the recently reported 1,2-diamination of alkenes.⁶⁸ Inspiration is gained from platinum-based anticancer complexes bearing chiral amine ligands that show differential activity against cancer.^{69–72} Considerations regarding the structure and stereoelectronic properties of chiral diamines are helpful in the design of new gold(III) diamine complexes. Moreover, the bicyclic property of diamine ligands can modulate the steric hindrance, stereoelectronic, nonplanarity, and lipophilic properties toward exciting new applications.⁷³ The chirality and optical properties of these complexes present new opportunities for catalysis, medicinal inorganic chemistry, and materials science.⁷⁰ In this work, the syntheses of four chiral Au(III) complexes bearing secondary diamine ligands are reported along with their complete spectroscopic characterization (^1H and ^{13}C NMR), and their purity was ascertained by high-performance liquid chromatography (HPLC)/electrospray ionization mass spectrometry (ESI-MS). The structures of these compounds were elucidated by X-ray crystallography.

RESULTS AND DISCUSSION

Norbornane-2,3-diamines are bicyclic, conformationally restricted compounds due to the decreased freedom of intramolecular rotations or motions around chemical bonds. The amino groups can be *cis* (usually both *exo*) or *trans* (one *exo* or one *endo*). The preparation of *cis* diamines has previously been achieved by the addition of N_2O_4 to norbornenes followed by reduction⁷⁴ or by double Curtius rearrangements of carboxylic acids;^{73,75} the preparation of *trans* diamines has been achieved by the nucleophilic attack of azides on aziridines followed by reduction.^{76,77} In our work, we prepared *cis*-2,3-norbornanediamine via a 1,3-dipolar cycloaddition between norbornene and an alkyl azide followed by N-alkylation and reduction.⁶⁸ We rationalized that structural modification to the cyclometalated $[\text{C}^{\text{N}}] \text{Au}(\text{III})$ framework with N-donor ancillary ligands that are conformationally restricted provides unique reactivity and stability. Diversification of cyclometalated Au(III) complexes bearing sterically or geometrically constrained ligands is attractive for exploring Au–macromolecular interactions, as well as unveiling new biological targets and reactivity for catalysis and material application. Cyclometalated $[\text{C}^{\text{N}}] \text{Au}(\text{III})$ systems supported with σ -donor diamino ligands are known to be stable.^{33,78} We previously reported Au(III) complexes bearing the primary diamine ligand *R,R*-DACH, and their stability and antiproliferative action were investigated.²⁴ Thus, we hypothesized that the use of secondary amines would enhance the complex stability. Here, we report the use of two different secondary

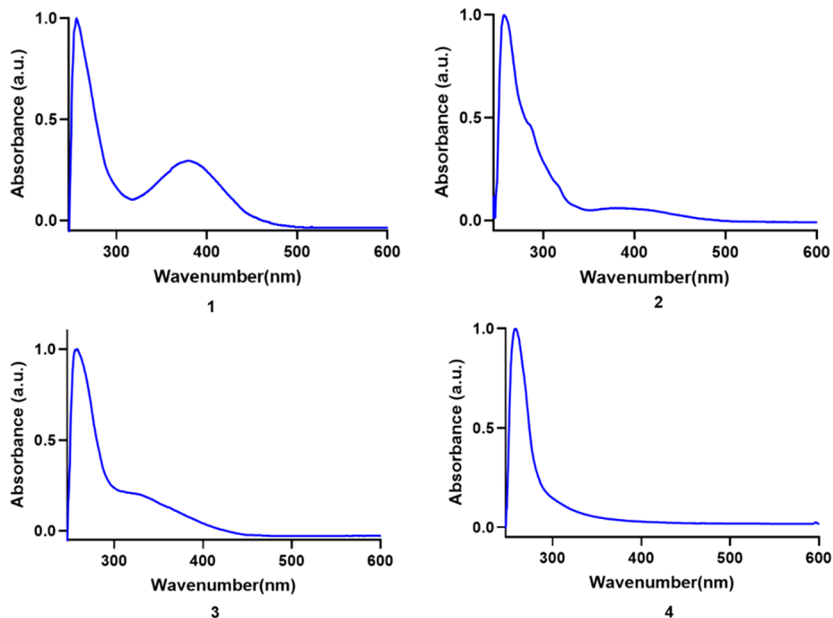


Figure 1. UV-vis absorption spectrum of complexes **1–4** in biologically relevant RPMI media at room temperature. The final concentration of the complexes was 50 μ M.

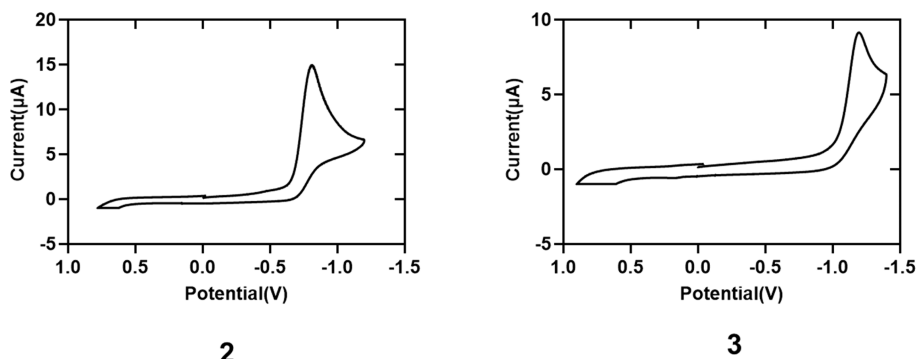


Figure 2. Cyclic voltammogram recorded at a platinum electrode in a DMSO solution of 10 mM **2** or **3** with a 0.10 M $\text{N}(\text{Bu})_4\text{PF}_6$ supporting electrolyte at a scan rate of 0.1 V/s using a Ag/AgCl reference electrode at room temperature.

diamine ligands that chelate Au(III) centers to form cationic complexes of the type $[\text{Au}^{\text{III}}\text{RN}^{\text{N}}\text{HNR}]^+$. The goal was to assess the impact of steric and electronic properties in the norbornane- or cyclohexyl-derived ligands on the complex stability and activity. To achieve monocationic Au(III) complexes, the reaction of cyclometalated $[\text{C}^{\text{N}}\text{N}]\text{Au}(\text{III})$ and diaminonorbornane was performed in an equimolar dichloromethane/methanol solution in the presence of a strong nonnucleophilic base, sodium *tert*-butoxide (NaOtBu), at room temperature for 16 h. The base deprotonates the diamine ligand following coordination to the Au center, and the deprotonation of the diamine ligand imparts a cationic state on the overall Au(III) complex (**Scheme 1**). When the Au(III) starting material with benzylpyridine was allowed to react with $(1R,2R)\text{-N}^1,\text{N}^2\text{-dibenzylcyclohexane-1,2-diamine}$, we optimized the conditions to use silver oxide (Ag_2O) instead of NaOtBu to minimize Au reduction and maximize yield (**Scheme 1**). The diamine ligands used formed a coordination bond (Au–N), with the Au(III) center trans to the sp^2 N of pyridine. The other N in the diamine ligand formed a covalent bond (Au–NH) with the Au(III) center and displayed chirality at the N, as shown by the X-ray crystal structure (**Figure 3**). All of the complexes were obtained in

good synthetic yields and displayed excellent stability when open to air and moisture.

Purification of the complexes was by normal-phase silica-gel flash chromatography using Teledyne Combi-Flash to afford a yellow powder for complexes **1**, **2**, and **4**. Complex **3**, which was prepared through the use of a silver-mediated reaction, was purified by filtration through an alumina pad, and the dichloromethane filtrate was precipitated with hexane. We found that complexes tolerated the purification conditions well with no observable degradation or reduction to elemental Au on the solid-phase silica or alumina. The purities of the compounds were ascertained by HPLC (**Figures S4, S8, S12, and S15**).

Complexes **1–4** were characterized by standard techniques, including UV-vis, NMR spectroscopy, ESI-MS, and cyclic voltammetry. The proton signals from the norbornane or cyclohexyl backbone were well resolved and located between 1.5 and 4.5 ppm as expected. The aromatic protons from the cyclometalated framework and benzyl units on the diamine ancillary ligand were at characteristic downfield regions of the ^1H NMR spectra.^{24,79,80} Electronic absorption profiles of **1–4** were measured in RPMI by UV-vis spectroscopy. All

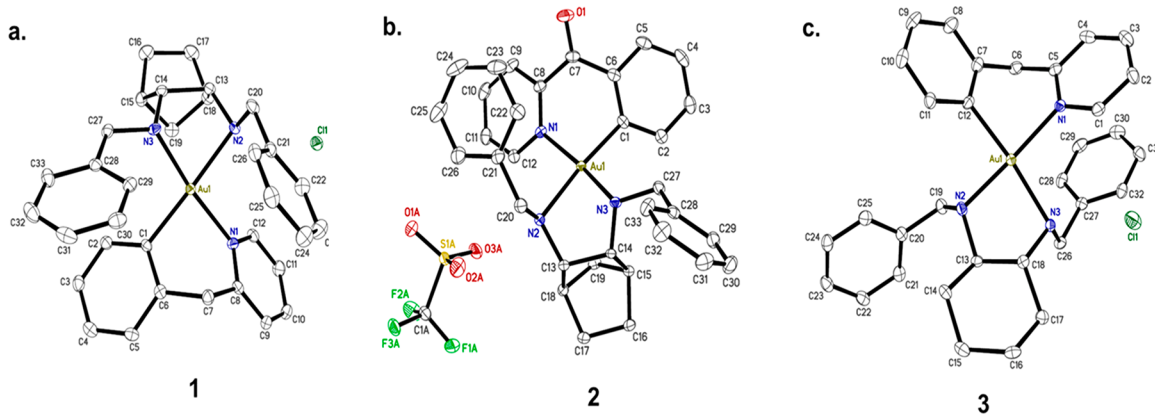


Figure 3. X-ray crystal structure of complexes 1–3, with ellipsoids drawn at 50%. Hydrogen atoms and solvents were omitted for clarity.

complexes display a characteristic high-energy band at 250 nm attributed to charge-transfer behavior. Except for complex 4, a red-shifted, low-energy peak in the range of 350–400 nm (λ_{max}) was observed for complexes 1–3 (Figure 1). Typically, high-energy absorption bands are often associated with π – π electronic transitions of metal-to-ligand or ligand-to-metal charge transfer.⁸¹ The oscillator strength and molecular orbital contributions obtained from time-dependent density functional theory calculations of other cyclometalated Au(III) compounds support the electronic transitions observed for 1–3.^{82–84} It is not clear as to why the low-energy bands were not observed for complex 4; absence of the bands may be associated with stability of 4 in RPMI.

The electrochemical behavior of 2 and 3 was examined by cyclic voltammetry in dimethyl sulfoxide (DMSO) using tetrabutylammonium hexafluorophosphate [$\text{N}(\text{Bu})_4\text{PF}_6$] as the supporting electrolyte, a platinum electrode, and Ag/AgCl as the reference electrode. We found that 2 bearing a norbornane ligand shows a major reduction event at about -0.8 V vs Ag/AgCl electrode (Figure 2). In the case of 3, which bears the cyclohexyl-derived ligand, the reduction event was at -1.1 V vs Ag/AgCl. The free diaminonorbornane ligand did not show redox activity, which strongly suggests that the observed reduction and oxidation events are Au(III)-complex-related. It is possible that the conformational restriction of the norbornane ligand imparts significant electrochemical stability to the Au(III) center in complex 2, compared to the cyclohexyl-derived ligand in complex 3. The result demonstrates the influence of restricted bicyclic ligands in tuning the redox behavior of cationic organogold complexes with potential benefits for stability under physiological conditions. Evidence for disproportionation in DMSO and reduction to metallic Au was not observed.

Using single-crystal X-ray diffraction, the structures of 1–3 were elucidated (Figure 3). Single crystals of 1–3 were grown by vapor diffusion as follows: (1) vapor diffusion of hexane into a concentrated CHCl_3 solution; (2) vapor diffusion of diethyl ether into a concentrated dichloromethane solution; (3) vapor diffusion of hexane into a concentrated dichloromethane solution. In complexes 1 and 2, all of the bond lengths around Au(III) have similar lengths except those of the Au–N (trans to pyridinium N) bonds, which were relatively shorter at 1.995 and 1.992, respectively. It is possible that the electronic contribution by diaminonorbornane influences the bond strength. The structures of the complexes show square-planar geometry around the Au(III) center. The triflate

counterion of complex 2 was from the diaminonorbornane synthesis via the azide–alkene cycloaddition.⁶⁸ The complex bearing the cyclohexyl-derived diamine 3 showed that all four bonds around the Au(III) center possess the same bond length (Table 1). Based on the X-ray crystal structures, the diamine

Table 1. Selected Interatomic Distances (Å) and Bond Angles (deg) from the X-ray Crystal Structures of 1–3

	1	2	3
Bond Length (Å)			
Au1–N1	2.077	2.0746	2.019
Au1–N2	2.141	2.1617	2.027
Au1–N3	1.995	1.992	2.107
Au1–C1	2.027	2.014	2.137
Bond Angle (deg)			
N3–Au1–Cl	101.12	98.74	90
N3–Au1–N1	173.11	171.23	177.39
C1–Au1–N1	85.66	88.42	87.4
N3–Au1–N2	76.68	75.61	83.73
C1–Au1–N2	177.8	174.05	173.36
N1–Au1–N2	96.54	97.38	98.86

ligands maintain an $\text{R}'\text{–S}'$ configuration in the norbornane Au(III) complex and an $\text{S}'\text{–S}'$ configuration for the cyclohexyl derivative.

Intrigued by the optical and electrochemical properties of conformationally restricted complexes 1 and 2, we subjected 1 to solution stability studies using RPMI media. We monitored the absorption signal of 1 by HPLC/ESI-MS over a 20 h period (Figure 4a). Briefly, a stock concentration of complex 1 was dissolved in RPMI, and at each time, aliquots of $100\ \mu\text{L}$ were taken and diluted with $100\ \mu\text{L}$ of methanol for LC/MS analysis. Complex 1 eluted at a retention time of 8 min ($A_{260\text{ nm}}$) with m/z 670.2, which remained unaltered throughout the study. The formation of other peaks was not observed, indicative of a soluble and perhaps physiologically stable complex. Encouraged by the stability of 1 in RPMI, we conducted a more rigorous physiological stability using the well-known biological reductant L-glutathione (L-GSH) and serum albumin, which is the most abundant protein in whole blood of most mammals, including humans. First, we incubated complex 1 with L-GSH in a 1:10 ratio, and using UV spectrophotometry, monitored the absorption bands (Figure S35). Changes to the absorption peak at 280 nm and the formation of a peak at 570 nm were observed by the 1

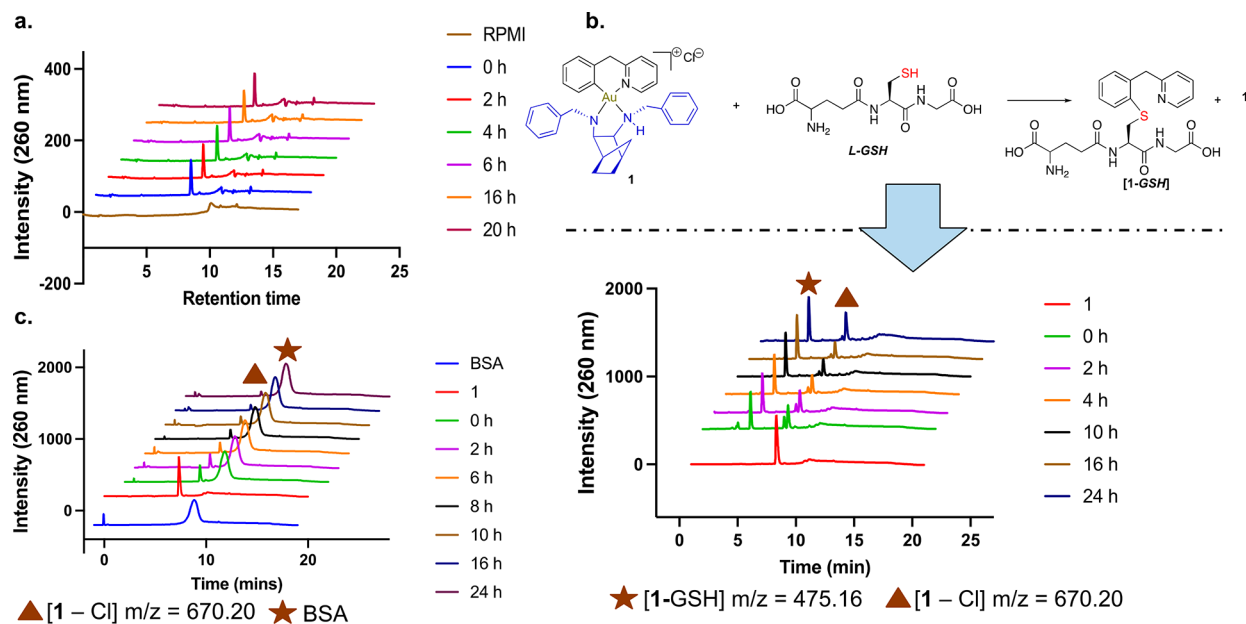


Figure 4. Stability studies. (A) HPLC trace (A_{260} nm) followed the incubation of **1** with a RPMI medium for 20 h. At respective time points, the reaction was aliquoted (100 μ L) and diluted with methanol (100 μ L) prior to HPLC runs. The blank run of RPMI/methanol is included to account for the baseline. (B) Formation of **1-GSH** by the chemical reaction of **1** and L-GSH as observed by LC/MS and monitored over a 24 h period. (C) HPLC trace (A_{260} nm) followed the incubation of **1** in methanol and BSA in phosphate-buffered saline for 24 h.

h time point, which remained unaltered until about 56 h. To further characterize this phenomenon, we used LC/ESI-MS to elucidate any potential speciation (Figure 4b) and found that, upon incubation of **1** with L-GSH, a reductively eliminated product of arylpyridine covalently linked to L-GSH through a C–S bond (**1-GSH**, m/z 475) forms together with intact complex **1** (m/z 670.2). It must be noted that cyclometalated Au(III) complexes of the C^N archetype can undergo reductive elimination to form C–S arylated products induced by thiol nucleophiles such as cysteines and proteins^{4,85–88} or direct C–N reductive elimination from Au(III).⁸⁹ Whereas the C–S transformation has been a useful bioorthogonal strategy in biological systems and important for target engagement by Au compounds, a careful balance of the reactivity and stability is needed for therapeutic development, making ligand tuning an important descriptor in Au-based probe/drug discovery. Interestingly, a significant amount of **1** remains intact in solution over the reaction period of 24 h. This suggests that **1** may maintain pharmacological activity and further demonstrates the utility of this class of compounds in a biological setting. Second, we studied the interaction of **1** with bovine serum albumin (BSA) in a reaction by UV spectrophotometry (Figure S35) and LC/ESI-MS (Figure 4c). While no major alterations were observed in the UV absorption profile over a 56 h reaction duration, the peak corresponding to complex **1** based on the retention time and m/z , although intact, diminishes over time but is observable at 24 h.

The antiproliferative potential of **1–4** was investigated in a panel of breast cancer cells (MDA-MB-231, MDA-MB-468, and MCF7) and an ovarian cancer cell line (A2780) by MTT assay (Table 2). The rationale for these cell lines was to evaluate the response of different cancer subtypes and respective metabolic statuses to **1–4**. In general, the conformationally restricted Au(III) complexes **1** and **2** were more potent with IC_{50} values of 1.6 and 4.2 μ M in glycolytic A2780 ovarian cancer cells, respectively. In the triple-negative

Table 2. Cell Viability of **1–4 Expressed as IC_{50} Values (μ M) in a Panel of Cancer Cells after 72 h of Treatment^a**

complex	IC_{50} (μ M)			
	MDA-MB 231 (breast)	MDA-MB 468 (breast)	MCF7 (breast)	A2780 (ovarian)
1	7.3 ± 0.04	28.8 ± 0.13	14.6 ± 0.04	1.6 ± 0.13
2	6.2 ± 0.02	13.5 ± 0.12	14.4 ± 0.03	4.2 ± 0.04
3	17.7 ± 0.03	97.1 ± 0.24	28.6 ± 0.03	4.7 ± 0.07
4	4.8 ± 0.03	12.7 ± 0.11	13.7 ± 0.03	5.2 ± 0.04

^aAu compounds were freshly prepared in DMSO and used immediately. The DMSO concentration was <1%.

breast cancer (TNBC) cell line, MDA-MB-231, which is dependent on both oxidative phosphorylation (OXPHOS) and glycolysis,⁹⁰ the IC_{50} values were 7.3 and 6.2 μ M for **1** and **2**, respectively. The recorded IC_{50} values extrapolated from dose–response curves for the cyclohexyl counterpart **3** were 2–4-fold higher in the breast cancer cells but maintained activity in the A2780 cells. Whereas compound **4** displayed activity across all cell lines, it was the least active in A2780 cells with an IC_{50} value of 5.2 μ M. It became clear that the OXPHOS-dependent TNBC cell line,⁹¹ MDA-MB-468, was not responsive to **1–4**. This observation may likely offer insights into the potential mechanism of action of these complexes, eliminating mitochondria as the major target.

In the context of structure activity relationship (SAR), we investigated the intracellular accumulation of **1–4** by measuring the Au content in A2780 cells (Figure 5). Briefly, A2780 cells were treated with the complexes at 5 or 10 μ M for 18 h, respectively, and graphite furnace atomic absorbance spectroscopy was used for Au quantification after washing of the cells and digestion. In the two treatment conditions used, it was clear that **2** was most taken up and **3** was the least taken up in the A2780 cells. The triflate counterion in **2** may potentiate physicochemical properties useful for enhanced cellular uptake. Moreover, the combination of benzylpyridine and the

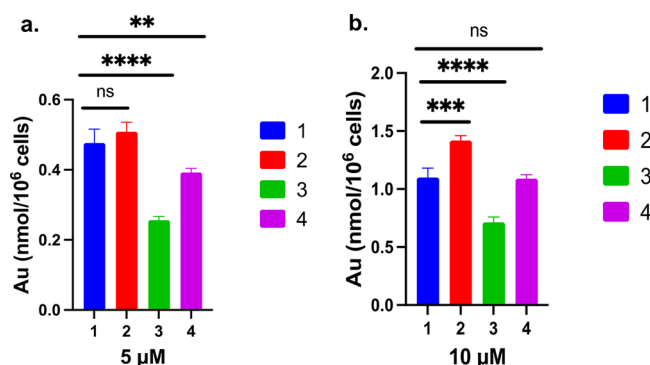


Figure 5. Cellular uptake. Intracellular accumulation of **1–4** in A2780 cancer cells. Cells were treated with (left) 5 or (right) 10 μ M for 18 h.

dibenzylcyclohexane-1,2-diamine ligand in **3** is not favorable for increased cellular uptake. This explains the relatively poor potency of **3** among the compound series evaluated. At a treatment concentration of 5 μ M, the cellular uptakes of **1** and **2** were comparable. Conceivably, the high uptake of **2** dictates the promising antiproliferative activity observed across multiple cell lines. From our studies, we notice that the conformationally restricted norbornane ligands enhance the electrochemical and solution stability of the overall Au(III) complex and demonstrate improved cellular uptake and anticancer potency in cells. Importantly, the use of benzylpyridine for cyclometalation as in **2** and **4** contributes to the uptake and antiproliferative action in cancer cells.

We used a fluorescence-assisted cell sorting study to assess the apoptotic potential of **1** in ovarian cells. The A2780 cells were treated with **1** at 5 μ M along with Annexin V/fluorescein isothiocyanate (FITC) and propidium iodide (Figure 6). The experiment showed that cells treated with **1** induced 15% apoptosis at 5 μ M in A2780 cells after 24 h of exposure compared to the control cells. The apoptotic phenotype was further verified by examining the critical markers of apoptosis via immunoblotting (Figure 6d). The accumulation of cleaved poly(ADP-ribose) polymerase (PARP) and depleted PARP in a concentration-dependent manner by 24 h supports an apoptotic mechanism. However, based on the minimal alteration to the cytochrome *c* expression, it is possible that apoptosis occurs via a cytochrome *c*-independent mechanism.⁹²

As demonstrated through electrochemical studies, the complexes under investigation are redox-active species;

therefore, we conducted flow cytometry studies to examine whether the redox activity of **1** produces total intracellular ROS (Figure 7a,b). In A2780 cells, cellular ROS increased in a dose-dependent manner, whereas *N*-acetylcysteine cotreatment largely reversed the effect. Mitochondrial ROS was undetectable using MitoSOX assay in a flow cytometry experiment (Figure 7c,d) measured under conditions similar to those of the total ROS study. The elevation of cellular ROS in A2780 by **1** is a critical driver of cell death.⁹³ Au complexes that evoke ROS-dependent mechanisms often exert thioredoxin inhibition as a probable cause of ROS accumulation, leading to oxidative stress. Taken together, these studies detail the total ROS specificity induced by **1** resulting in cell death. Further studies beyond the scope of this report are needed to characterize the molecular target(s) of this class of compounds.

Initial cell viability studies showed that OXPHOS-dependent cells do not respond well to complexes **1–4**. To assess the effect of conformationally restricted compounds on mitochondrial-related toxicity, as induced by other Au(III) agents,⁹⁴ we evaluated the effect of **1** on mitochondrial function and glycolysis⁹⁵ in A2780 cells. Using a seahorse extracellular flux analyzer (Seahorse XF96)⁹⁶ A2780 cells were subjected to the cell mito stress test that measures mitochondrial respiration and concomitant glycolytic effects (Figure 8a,b). Briefly, cells were pretreated with **1** for 12 h followed by mitochondrial complex inhibitors (oligomycin, rotenone, and antimycin A) or uncoupler [carbonyl cyanide-4-(trifluoromethoxy)-phenylhydrazone] to measure the oxygen consumption rate (OCR), extracellular acidification rate (ECAR), and other extrapolated parameters such as basal respiration, maximal respiration, and proton leak that characterize mitochondrial stress.⁹⁷ We found that the measure of mitochondrial respiration, which is the OCR, was not significantly affected by the pretreatment of **1** in A2780 cells (Figure 8a). Further, extrapolated mitochondrial parameters including basal respiration and maximal respiration remained unaltered (Figure S38).⁹⁸ Additionally, the spare reserve capacity (SRC) is a robust functional readout to evaluate the mitochondrial reserve in nontransformed and cancer cells.⁹⁹ The SRC in A2780 cells decreased following the treatment of **1** at 10 μ M. The coupling efficiency in response to **1** followed a pattern similar to that of the adenosine triphosphate (ATP) parameter, with no changes at higher concentrations in comparison to control cells, pointing to unaltered mitochondrial metabolism by **1** in A2780 cancer cells. ECAR, which is often a measure of the glycolytic performance, was activated by **1** at 10 μ M in A2780

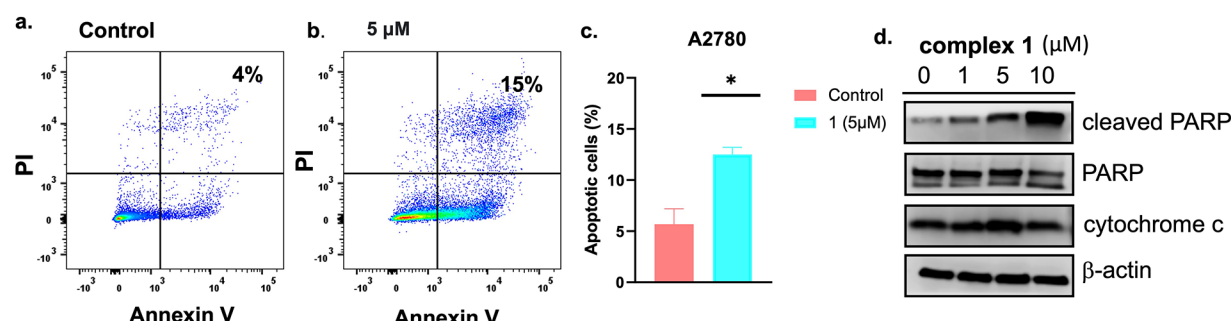


Figure 6. Dual-staining flow cytometry experiment showing apoptosis at 5 μ M **1** in A2780 cells for 24 h. Propidium iodide and FITC-labeled Annexin V were used to detect apoptotic populations: (a) control; (b) treated by complex **1**. (c) Bar chart representation of the apoptotic populations extrapolated from parts a and b. Data analyzed by a two-tailed unpaired Student's *t* test (*, $p < 0.05$). (d) Expression levels of apoptotic proteins in A2780 following a 24 h treatment of **1** at the indicated concentrations.

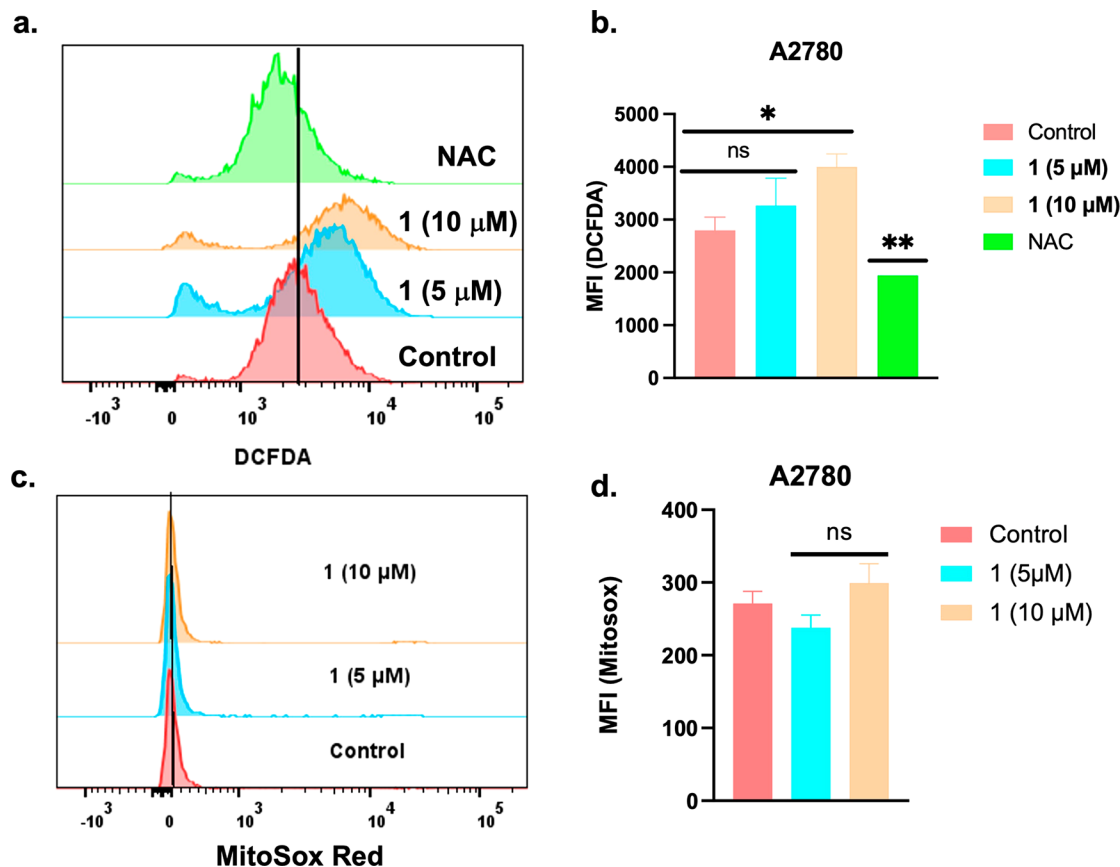


Figure 7. (a) Total intracellular ROS levels induced by **1** using DCFDA ($(H_2DCFDA = 2',7'$ -dichlorodihydrofluorescein diacetate) flow cytometry assay. (b) Bar chart representation of data extrapolated from part a. (c) Mitochondrial ROS measured by MitoSOX flow cytometry (PE channel) assay. (d) Bar chart representation of data extrapolated from part c. Cells were exposed to complex **1** for 2 h prior to assay. Data are plotted as the mean \pm SD ($n = 3$). Data were analyzed by ordinary one-way ANOVA followed by Dunnett's multiple comparison test and a two-tailed unpaired Student's *t* test (**, $p < 0.01$; *, $p < 0.05$; n.s. = not significant).

cells (Figure 8b) with a dose-dependent increase in the nonmitochondrial OCR, further confirming our hypothesis that this class of conformationally restricted Au(III) complexes adopts a mechanism-of-action independent of mitochondrial modulation. Functional studies using the mitochondrial membrane potential (MMP) showed that **1** does not depolarize MMP in tetramethylrhodamine ethyl ester (TMRE)-based flow cytometry studies (Figure 8c,d). Overall, these studies verify that compound **1** does not induce mitochondrial dysfunction in cancer cells.

CONCLUSION

In summary, a new cyclometalated Au(III) scaffold supported by conformationally restricted bicyclic norbornane ligands has been synthesized. The characterization of these chiral complexes reveals monomeric Au(III) species generated by coordinating chiral diamine ligands to the Au center. Interestingly, these reactions proceed by ligand substitution of the chlorido ligands on the starting cyclometalated Au(III) scaffolds. The spatial arrangement of the ligand surrounding the Au center was confirmed by X-ray crystallography. The unique chirality at the N center covalently bonded to Au (NH-Au) presents additional chiral complexity to the overall Au(III) complex. It is worth mentioning that these complexes are air- and moisture-stable. This new structural class of Au(III) compounds provides a platform for new synthetic materials

that will be beneficial to catalysis, biological probe development, therapeutics, and materials science.

The stability of complex **1** in RPMI media and the relative stability in the presence of a biological reductant or protein, point to the biological relevance of these scaffolds. *In vitro*, all four complexes were more cytotoxic in glycolysis-dependent cell lines compared with cells that are highly dependent on oxidative phosphorylation. Unlike other Au anticancer agents previously developed in our laboratory and others, the initial cell viability studies prompted a potentially different mechanism of action independent of the mitochondrial function. An increase in the apoptotic population was observed after treatment with **1**, an effect we attribute to increased oxidative stress induced in A2780 cells. We also noted that the induction of ROS by **1** was in cellular locations other than the mitochondria because no significant increase in mitochondrial ROS was observed.

Investigating the mitochondrial bioenergetics of A2780 cells pretreated with **1** showed perturbation of the glycolysis rate of the cells, while the OCR remained relatively unchanged. Taken together, tuning the organogold center with conformationally restricted bicyclic diamines exerts a different biological consequence independent of mitochondrial dysfunction. Further investigation beyond the scope of this report is, however, required to fully characterize the mechanism of anticancer action of this new class of compounds.

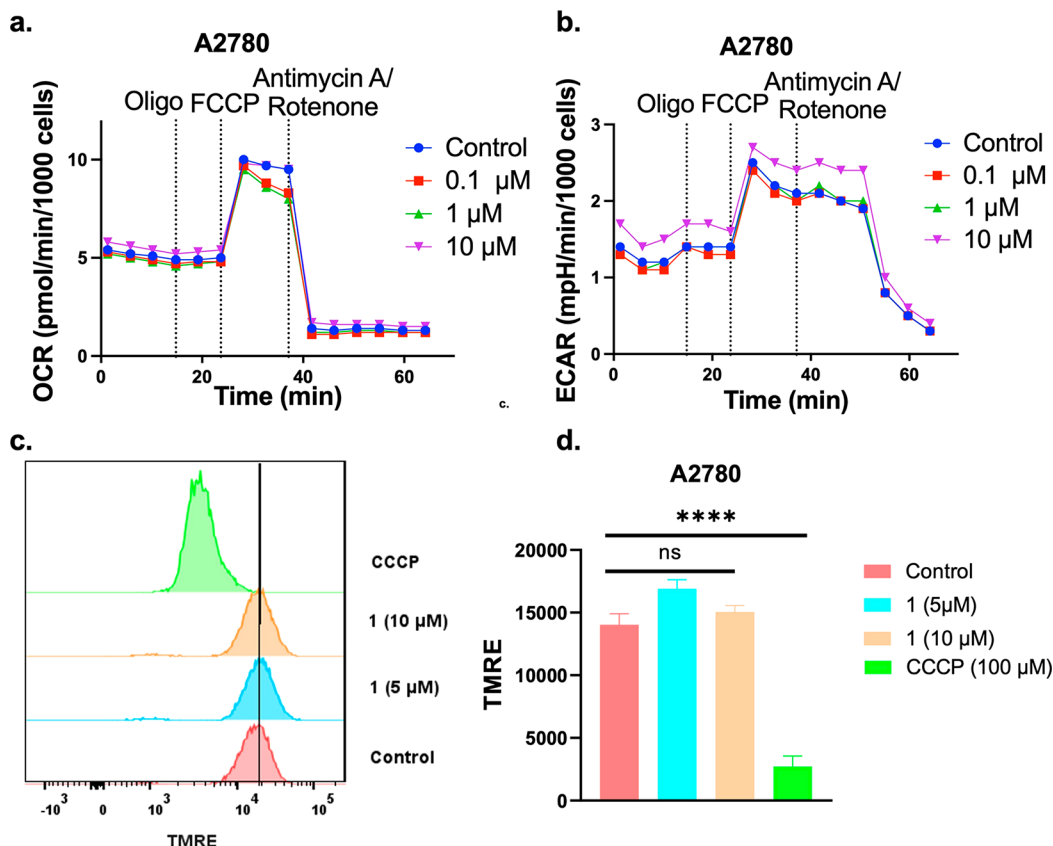


Figure 8. (a) OCR from a cell mito stress study using Seahorse XF96. A2780 cancer cells were pretreated with **1** (12 h), and various inhibitors of electron transport chain (ETC) were added at indicated time points. (b) ECAR from a cell mito stress study using Seahorse XF96. A2780 cancer cells were pretreated with **1** (12 h), and various inhibitors of ETC were added at indicated time points. (c) Mitochondria membrane potential measured by flow cytometry analysis of the TMRE fluorescence intensity. (d) Bar chart of MMP extrapolated from part c. Data are plotted as the mean \pm SD ($n = 3$). Data were analyzed by ordinary one-way ANOVA followed by Dunnett's multiple comparison test (****, $p < 0.0001$; n.s. = not significant).

The SAR studies further outline the impact of conformationally restricted norbornane ligands on the electrochemical and solution stability of the overall Au(III) complex and potentiate the cellular uptake and anticancer potency in cells, as demonstrated by **1**. Notably, the use of benzylpyridine for cyclometalation, as in **2** and **4**, influences the uptake and antiproliferative action in cancer cells. Overall, conformationally restricted ligands may pave the way toward a more diverse class of biologically relevant Au(III) complexes.

ASSOCIATED CONTENT

Supporting Information

The Supporting Information is available free of charge at <https://pubs.acs.org/doi/10.1021/acs.inorgchem.3c02066>.

Crystal data and structure refinement for compounds **1**–**3**, ¹H and ¹³C NMR spectra, HPLC traces, ESI-MS, electrochemistry, and UV–vis spectra for complexes, and dose-response graphs for complexes and mito stress assay parameters (PDF)

Accession Codes

CCDC 2248360–2248362 contain the supplementary crystallographic data for this paper. These data can be obtained free of charge via www.ccdc.cam.ac.uk/data_request/cif, or by emailing data_request@ccdc.cam.ac.uk, or by contacting The Cambridge Crystallographic Data Centre, 12 Union Road, Cambridge CB2 1EZ, UK; fax: +44 1223 336033.

AUTHOR INFORMATION

Corresponding Author

Samuel G. Awuah – Department of Chemistry, University of Kentucky, Lexington, Kentucky 40506, United States; Center for Pharmaceutical Research and Innovation and Department of Pharmaceutical Sciences, College of Pharmacy University of Kentucky, Lexington, Kentucky 40536, United States; Markey Cancer Center, University of Kentucky, Lexington, Kentucky 40536, United States; orcid.org/0000-0003-4947-7283; Email: awuah@uky.edu

Authors

Sailajah Gukathasan – Department of Chemistry, University of Kentucky, Lexington, Kentucky 40506, United States

Oluwatosin A. Obisesan – Department of Chemistry, University of Kentucky, Lexington, Kentucky 40506, United States

Setareh Saryazdi – Department of Chemistry, University of Kentucky, Lexington, Kentucky 40506, United States

Libby Ratliff – Department of Chemistry, University of Kentucky, Lexington, Kentucky 40506, United States; orcid.org/0000-0002-0187-9921

Sean Parkin – Department of Chemistry, University of Kentucky, Lexington, Kentucky 40506, United States

Robert B. Grossman – Department of Chemistry, University of Kentucky, Lexington, Kentucky 40506, United States; orcid.org/0000-0001-8866-3754

Complete contact information is available at:
<https://pubs.acs.org/10.1021/acs.inorgchem.3c02066>

Notes

The authors declare the following competing financial interest(s): S.G.A. has patents pending to University of Kentucky Research Foundation. S.G.A. serves on the advisory board and is Chief Science Officer for Phronesis AI.

ACKNOWLEDGMENTS

We are grateful for financial support from the National Cancer Institute (NCI) R01CA258421-01 (to S.G.A.) and a National Science Foundation Chemistry of Life Processes (NSF-CLP) grant for S.G.A. (Award CHE-2203559). We thank the following facilities at the University of Kentucky, who provided support in completion of the experiments detailed in this paper: The UK NMR Center supported by the NSF (CHE-997738) and the UK X-ray facility supported by the MRI program from the NSF (CHE-1625732). For the flow cytometry experiments, we thank UK Flow Cytometry and Immune Function core supported by the Office of the Vice President of Research, Markey Cancer Center, and NCI Center Core Support Grant (P30 CA177558). We also thank Dr. Pat Sullivan's laboratory for access to their Seahorse XF96 and Dr. Hemendra Vekaria for running mito stress experiments.

REFERENCES

- (1) Jürgens, S.; Scalcon, V.; Estrada-Ortiz, N.; Folda, A.; Tonolo, F.; Jandl, C.; Browne, D. L.; Rigobello, M. P.; Kühn, F. E.; Casini, A. Exploring the C⁺N⁺C theme: Synthesis and biological properties of tridentate cyclometalated gold(III) complexes. *Bioorg. Med. Chem.* **2017**, *25* (20), 5452–5460.
- (2) Martín, J.; Gómez-Benrga, E.; Genoux, A.; Nevado, C. Synthesis of Cyclometalated Gold(III) Complexes via Catalytic Rhodium to Gold(III) Transmetalation. *Angew. Chem., Int. Ed. Engl.* **2022**, *61* (20), e202116755.
- (3) Gukathasan, S.; Awuah, S. G. Synthetic Strategies for the Preparation of Gold-based Anticancer Agents. *Encyclopedia of Inorganic and Bioinorganic Chemistry* **2022**, 1–32.
- (4) Bonsignore, R.; Thomas, S. R.; Rigoulet, M.; Jandl, C.; Pöthig, A.; Bourissou, D.; Barone, G.; Casini, A. C-C Cross-Couplings from a Cyclometalated Au(III) C \wedge N Complex: Mechanistic Insights and Synthetic Developments. *Chemistry* **2021**, *27* (57), 14322–14334.
- (5) Rocchigiani, L.; Bochmann, M. Recent Advances in Gold(III) Chemistry: Structure, Bonding, Reactivity, and Role in Homogeneous Catalysis. *Chem. Rev.* **2021**, *121* (14), 8364–8451.
- (6) Thomas, S. R.; Casini, A. Gold compounds for catalysis and metal-mediated transformations in biological systems. *Curr. Opin. Chem. Biol.* **2020**, *55*, 103–110.
- (7) Tang, M.-C.; Chan, M.-Y.; Yam, V. W.-W. Molecular Design of Luminescent Gold(III) Emitters as Thermally Evaporable and Solution-Processable Organic Light-Emitting Device (OLED) Materials. *Chem. Rev.* **2021**, *121* (13), 7249–7279.
- (8) Tang, M. C.; Chan, A. K.; Chan, M. Y.; Yam, V. W. W. Platinum and Gold Complexes for OLEDs. *Top Curr. Chem. (Cham)* **2016**, *374* (4), 46.
- (9) Ofori, S.; Gukathasan, S.; Awuah, S. G. Gold-Based Pharmacophore Inhibits Intracellular MYC Protein. *Chemistry* **2021**, *27* (12), 4168–4175.
- (10) Gukathasan, S.; Parkin, S.; Black, E. P.; Awuah, S. G. Tuning Cyclometalated Gold(III) for Cysteine Arylation and Ligand-Directed Bioconjugation. *Inorg. Chem.* **2021**, *60* (19), 14582–14593.
- (11) Ko, H.-M.; Deng, J.-R.; Cui, J.-F.; Kung, K. K.-Y.; Leung, Y.-C.; Wong, M.-K. Selective modification of alkyne-linked peptides and proteins by cyclometalated gold(III) (C⁺N⁺) complex-mediated alkynylation. *Bioorg. Med. Chem.* **2020**, *28* (7), 115375.
- (12) Berners-Price, S. J.; Filipovska, A. Gold compounds as therapeutic agents for human diseases. *Metallomics* **2011**, *3* (9), 863–873.
- (13) Zhang, J.; Li, Y.; Fang, R.; Wei, W.; Wang, Y.; Jin, J.; Yang, F.; Chen, J. Organometallic gold(I) and gold(III) complexes for lung cancer treatment. *Front. Pharmacol.* **2022**, *13*. DOI: 10.3389/fphar.2022.979951
- (14) Khan, H. A.; Al-Hoshani, A.; Isab, A. A.; Alhomida, A. S. A Gold(III) Complex with Potential Anticancer Properties. *ChemistrySelect* **2022**, *7* (45), e202202956.
- (15) Todorov, L.; Kostova, I. Recent Trends in the Development of Novel Metal-Based Antineoplastic Drugs. *Molecules* **2023**, *28* (4), 1959.
- (16) Zhang, J.; Jiang, M.; Li, S.; Zhang, Z.; Sun, H.; Yang, F.; Liang, H. Developing a Novel Anticancer Gold(III) Agent to Integrate Chemotherapy and Immunotherapy. *J. Med. Chem.* **2021**, *64* (10), 6777–6791.
- (17) Mertens, R. T.; Gukathasan, S.; Arojojoye, A. S.; Olelewe, C.; Awuah, S. G. Next Generation Gold Drugs and Probes: Chemistry and Biomedical Applications. *Chem. Rev.* **2023**, *123* (10), 6612–6667.
- (18) Chaffman, M.; Brogden, R. N.; Heel, R. C.; Speight, T. M.; Avery, G. S. Auranofin. *Drugs* **1984**, *27* (5), 378–424.
- (19) Müllegger, S.; Schöberger, W.; Rashidi, M.; Lengauer, T.; Klappenberger, F.; Diller, K.; Kara, K.; Barth, J. V.; Rauls, E.; Schmidt, W. G.; Koch, R. Preserving charge and oxidation state of Au(III) ions in an agent-functionalized nanocrystal model system. *ACS Nano* **2011**, *5* (8), 6480–6486.
- (20) Wu, C. Y.; Horibe, T.; Jacobsen, C. B.; Toste, F. D. Stable gold(III) catalysts by oxidative addition of a carbon-carbon bond. *Nature* **2015**, *517* (7535), 449–454.
- (21) Lee, J. S.; Kapustin, E. A.; Pei, X.; Llopis, S.; Yaghi, O. M.; Toste, F. D. Architectural Stabilization of a Gold(III) Catalyst in Metal-Organic Frameworks. *Chem.* **2020**, *6* (1), 142–152.
- (22) Carretero, S.; Corma, A.; Iglesias, M.; Sánchez, F. Stabilization of Au(III) on heterogeneous catalysts and their catalytic similarities with homogeneous Au(III) metal organic complexes. *Appl. Catal. A: Gen.* **2005**, *291* (1), 247–252.
- (23) Kung, K. K.-Y.; Ko, H.-M.; Cui, J.-F.; Chong, H.-C.; Leung, Y.-C.; Wong, M.-K. Cyclometalated gold(III) complexes for chemoselective cysteine modification via ligand controlled C-S bond-forming reductive elimination. *Chem. Commun.* **2014**, *50* (80), 11899–11902.
- (24) Gukathasan, S.; Parkin, S.; Awuah, S. G. Cyclometalated Gold(III) Complexes Bearing DACH Ligands. *Inorg. Chem.* **2019**, *58* (14), 9326–9340.
- (25) Rekhroukh, F.; Brousses, R.; Amgoune, A.; Bourissou, D. Cationic Gold(III) Alkyl Complexes: Generation, Trapping, and Insertion of Norbornene. *Angew. Chem., Int. Ed. Engl.* **2015**, *54* (4), 1266–1269.
- (26) von Wachenfeldt, H.; Polukeev, A. V.; Loganathan, N.; Paulsen, F.; Röse, P.; Garreau, M.; Wendt, O. F.; Strand, D. Cyclometallated gold(III) aryl-pyridine complexes as efficient catalysts for three-component synthesis of substituted oxazoles. *Dalton Trans.* **2015**, *44* (12), 5347–5353.
- (27) Au, V. K.-M.; Wong, K. M.-C.; Zhu, N.; Yam, V. W.-W. Luminescent Cyclometalated Dialkynylgold(III) Complexes of 2-Phenylpyridine-Type Derivatives with Readily Tunable Emission Properties. *Chem. Eur. J.* **2011**, *17* (1), 130–142.
- (28) Serra, J.; Font, P.; Sosa Carrizo, E. D.; Mallet-Ladeira, S.; Massou, S.; Parella, T.; Miqueu, K.; Amgoune, A.; Ribas, X.; Bourissou, D. Cyclometalated gold(III) complexes: noticeable differences between (N,C) and (P,C) ligands in migratory insertion. *Chem. Sci.* **2018**, *9* (16), 3932–3940.
- (29) Arojojoye, A. S.; Olelewe, C.; Gukathasan, S.; Kim, J. H.; Vekaria, H.; Parkin, S.; Sullivan, P. G.; Awuah, S. G. Serum-Stable Gold(III) Bisphosphine Complex Induces Mild Mitochondrial

Uncoupling and In Vivo Antitumor Potency in Triple Negative Breast Cancer. *J. Med. Chem.* **2023**, *66*, 7868.

(30) Kung, K. K.-Y.; Lo, V. K.-Y.; Ko, H.-M.; Li, G.-L.; Chan, P.-Y.; Leung, K.-C.; Zhou, Z.; Wang, M.-Z.; Che, C.-M.; Wong, M.-K. Cyclometallated Gold(III) Complexes as Effective Catalysts for Synthesis of Propargylic Amines, Chiral Allenes and Isoxazoles. *Adv. Synth. Catal.* **2013**, *355* (10), 2055–2070.

(31) Kim, J. H.; Ofori, S.; Parkin, S.; Vekaria, H.; Sullivan, P. G.; Awuah, S. G. Anticancer gold(III)-bisphosphine complex alters the mitochondrial electron transport chain to induce in vivo tumor inhibition. *Chem. Sci.* **2021**, *12* (21), 7467–7479.

(32) Hyun Kim, J.; Ofori, S.; Mertens, R. T.; Parkin, S.; Awuah, S. G. Water-Soluble Gold(III)–Metformin Complex Alters Mitochondrial Bioenergetics in Breast Cancer Cells. *ChemMedChem* **2021**, *16* (20), 3222–3230.

(33) Navarro, M.; Tabey, A.; Szalóki, G.; Mallet-Ladeira, S.; Bourissou, D. Stable Au(III) Complexes Bearing Hemilabile P^N and C^N Ligands: Coordination of the Pendant Nitrogen upon Oxidation of Gold. *Organometallics* **2021**, *40* (11), 1571–1576.

(34) Reiersolmoen, A. C.; Battaglia, S.; Orthaber, A.; Lindh, R.; Erdélyi, M.; Fiksdahl, A. P,N-Chelated Gold(III) Complexes: Structure and Reactivity. *Inorg. Chem.* **2021**, *60* (5), 2847–2855.

(35) Kumar, R.; Nevado, C. Cyclometalated Gold(III) Complexes: Synthesis, Reactivity, and Physicochemical Properties. *Angew. Chem., Int. Ed.* **2017**, *56* (8), 1994–2015.

(36) Levchenko, V. A.; Siah, H.-S. M.; Øien-Ødegaard, S.; Kaur, G.; Fiksdahl, A.; Tilset, M. Catalytic studies of cyclometalated gold(III) complexes and their related UiO-67 MOF. *Mol. Catal.* **2020**, *492*, 111009.

(37) Bohan, P. T.; Toste, F. D. Well-Defined Chiral Gold(III) Complex Catalyzed Direct Enantioconvergent Kinetic Resolution of 1,5-Enynes. *J. Am. Chem. Soc.* **2017**, *139* (32), 11016–11019.

(38) Reid, J. P.; Hu, M.; Ito, S.; Huang, B.; Hong, C. M.; Xiang, H.; Sigman, M. S.; Toste, F. D. Strategies for remote enantiocontrol in chiral gold(III) complexes applied to catalytic enantioselective γ,δ -Diels–Alder reactions. *Chem. Sci.* **2020**, *11* (25), 6450–6456.

(39) Casini, A.; Thomas, S. R. The Beauty of Gold: Knowledge of Mechanisms Leads to Different Applications of Organogold Compounds in Medicine and Catalysis. *Chem. Lett.* **2021**, *50* (8), 1516–1522.

(40) Malmberg, R.; Venkatesan, K. Recent Advances in the Development of Blue and Deep-Blue Emitting Gold(I) and Gold(III) Molecular Systems. *Eur. J. Inorg. Chem.* **2021**, *2021* (47), 4890–4902.

(41) Leung, M.-Y.; Leung, S. Y.-L.; Yim, K.-C.; Chan, A. K.-W.; Ng, M.; Yam, V. W.-W. Multiresponsive Luminescent Cationic Cyclometalated Gold(III) Amphiphiles and Their Supramolecular Assembly. *J. Am. Chem. Soc.* **2019**, *141* (49), 19466–19478.

(42) To, W.-P.; Tong, G. S. M.; Cheung, C.-W.; Yang, C.; Zhou, D.; Che, C.-M. Luminescent Cyclometalated Gold(III) Alkyl Complexes: Photophysical and Photochemical Properties. *Inorg. Chem.* **2017**, *56* (9), 5046–5059.

(43) Malmberg, R.; Venkatesan, K. Conceptual advances in the preparation and excited-state properties of neutral luminescent (C^NN) and (C^NC^{*}) monocyclometalated gold(III) complexes. *Coord. Chem. Rev.* **2021**, *449*, 214182.

(44) Tsai, J. L.-L.; Chan, A. O.-Y.; Che, C.-M. A luminescent cyclometalated gold(III)–avidin conjugate with a long-lived emissive excited state that binds to proteins and DNA and possesses anti-proliferation capacity. *Chem. Commun.* **2015**, *51* (40), 8547–8550.

(45) Zou, T.; Lum, C. T.; Chui, S. S.-Y.; Che, C.-M. Gold(III) Complexes Containing N-Heterocyclic Carbene Ligands: Thiol “Switch-on” Fluorescent Probes and Anti-Cancer Agents. *Angew. Chem., Int. Ed.* **2013**, *52* (10), 2930–2933.

(46) Luo, H.; Cao, B.; Chan, A. S. C.; Sun, R. W.-Y.; Zou, T. Cyclometalated Gold(III)-Hydride Complexes Exhibit Visible Light-Induced Thiol Reactivity and Act as Potent Photo-Activated Anti-Cancer Agents. *Angew. Chem., Int. Ed.* **2020**, *59* (27), 11046–11052.

(47) Fung, S. K.; Zou, T.; Cao, B.; Lee, P. Y.; Fung, Y. M.; Hu, D.; Lok, C. N.; Che, C. M. Cyclometalated Gold(III) Complexes Containing N-Heterocyclic Carbene Ligands Engage Multiple Anti-Cancer Molecular Targets. *Angew. Chem., Int. Ed. Engl.* **2017**, *56* (14), 3892–3896.

(48) Carboni, S.; Zucca, A.; Stoccoro, S.; Maiore, L.; Arca, M.; Ortú, F.; Artner, C.; Keppler, B. K.; Meier-Menches, S. M.; Casini, A.; Cinelli, M. A. New Variations on the Theme of Gold(III) C^NN Cyclometalated Complexes as Anticancer Agents: Synthesis and Biological Characterization. *Inorg. Chem.* **2018**, *57* (23), 14852–14865.

(49) Bertrand, B.; Williams, M. R. M.; Bochmann, M. Gold(III) Complexes for Antitumor Applications: An Overview. *Chem. Eur. J.* **2018**, *24* (46), 11840–11851.

(50) Zhou, X.-Q.; Carbo-Bague, I.; Siegler, M. A.; Hilgendorf, J.; Basu, U.; Ott, I.; Liu, R.; Zhang, L.; Ramu, V.; Ijzerman, A. P.; Bonnet, S. Rollover Cyclometalation vs Nitrogen Coordination in Tetrapyridyl Anticancer Gold(III) Complexes: Effect on Protein Interaction and Toxicity. *JACS Au* **2021**, *1* (4), 380–395.

(51) Zou, T.; Lum, C. T.; Lok, C.-N.; Zhang, J.-J.; Che, C.-M. Chemical biology of anticancer gold(III) and gold(I) complexes. *Chem. Soc. Rev.* **2015**, *44* (24), 8786–8801.

(52) Frik, M.; Fernández-Gallardo, J.; Gonzalo, O.; Mangas-Sanjuan, V.; González-Alvarez, M.; Serrano del Valle, A.; Hu, C.; González-Alvarez, I.; Bermejo, M.; Marzo, I.; Contel, M. Cyclometalated Iminophosphorane Gold(III) and Platinum(II) Complexes. A Highly Permeable Cationic Platinum(II) Compound with Promising Anticancer Properties. *J. Med. Chem.* **2015**, *58* (15), 5825–5841.

(53) Massai, L.; Cirri, D.; Michelucci, E.; Bartoli, G.; Guerri, A.; Cinelli, M. A.; Cocco, F.; Gabbiani, C.; Messori, L. Organogold(III) compounds as experimental anticancer agents: chemical and biological profiles. *Biometals* **2016**, *29* (5), 863–872.

(54) Coronello, M.; Mini, E.; Caciagli, B.; Cinelli, M. A.; Bindoli, A.; Gabbiani, C.; Messori, L. Mechanisms of cytotoxicity of selected organogold(III) compounds. *J. Med. Chem.* **2005**, *48* (21), 6761–6765.

(55) Gabbiani, C.; Cinelli, M. A.; Maiore, L.; Massai, L.; Scaletti, F.; Messori, L. Chemistry and biology of three representative gold(III) compounds as prospective anticancer agents. *Inorg. Chim. Acta* **2012**, *393*, 115–124.

(56) Mertens, R. T.; Parkin, S.; Awuah, S. G. Cancer cell-selective modulation of mitochondrial respiration and metabolism by potent organogold(III) dithiocarbamates. *Chem. Sci.* **2020**, *11* (38), 10465–10482.

(57) Khodjoyan, S.; Remadna, E.; Dossmann, H.; Lesage, D.; Gontard, G.; Forté, J.; Hoffmeister, H.; Basu, U.; Ott, I.; Spence, P.; Waller, Z. A. E.; Salmain, M.; Bertrand, B. [(C₆H₅)Au(N₃N₃)]⁺ Complexes as a New Family of Anticancer Candidates: Synthesis, Characterization and Exploration of the Antiproliferative Properties. *Chem. Eur. J.* **2021**, *27* (63), 15773–15785.

(58) Fan, D.; Yang, C.-T.; Ranford, J. D.; Vittal, J. J. Chemical and biological studies of gold(III) complexes with uninegative bidentate N–N ligands. *Dalton Trans.* **2003**, *24*, 4749–4753.

(59) Lu, Y.; Ma, X.; Chang, X.; Liang, Z.; Lv, L.; Shan, M.; Lu, Q.; Wen, Z.; Gust, R.; Liu, W. Recent development of gold(I) and gold(III) complexes as therapeutic agents for cancer diseases. *Chem. Soc. Rev.* **2022**, *51* (13), 5518–5556.

(60) Malmberg, R.; Bachmann, M.; Blacque, O.; Venkatesan, K. Thermally Robust and Tuneable Phosphorescent Gold(III) Complexes Bearing (N^NN)-Type Bidentate Ligands as Ancillary Chelates. *Chemistry* **2019**, *25* (14), 3627–3636.

(61) Jouhannet, R.; Dagorne, S.; Blanc, A.; Frémont, P. Chiral Gold(III) Complexes: Synthesis, Structure, and Potential Applications. *Chem. Eur. J.* **2021**, *27* (36), 9218–9240.

(62) Arojojoye, A. S.; Kim, J. H.; Olelewe, C.; Parkin, S.; Awuah, S. G. Chiral gold(III) complexes: speciation, *in vitro*, and *in vivo* anticancer profile. *Chem. Commun.* **2022**, *58* (73), 10237–10240.

(63) Jiang, J.-J.; Wong, M.-K. Recent Advances in the Development of Chiral Gold Complexes for Catalytic Asymmetric Catalysis. *Chem. Asian J.* **2021**, *16* (5), 364–377.

(64) Zhang, J.-J.; Sun, R. W.-Y.; Che, C.-M. A dual cytotoxic and anti-angiogenic water-soluble gold(III) complex induces endoplasmic reticulum damage in HeLa cells. *Chem. Commun.* **2012**, *48* (28), 3388–3390.

(65) Babak, M. V.; Chong, K. R.; Rapta, P.; Zannikou, M.; Tang, H. M.; Reichert, L.; Chang, M. R.; Kushnarev, V.; Heffeter, P.; Meier-Menches, S. M.; Lim, Z. C.; Yap, J. Y.; Casini, A.; Balyasnikova, I. V.; Ang, W. H. Interfering with Metabolic Profile of Triple-Negative Breast Cancers Using Rationally Designed Metformin Prodrugs. *Angew. Chem., Int. Ed.* **2021**, *60* (24), 13405–13413.

(66) Nova, A.; Balcells, D. Does the metal protect the ancillary ligands? C–H strengthening and deactivation in amines and phosphines upon metal-binding. *Chem. Commun.* **2014**, *50* (5), 614–616.

(67) Haas, K. L.; Franz, K. J. Application of Metal Coordination Chemistry To Explore and Manipulate Cell Biology. *Chem. Rev.* **2009**, *109* (10), 4921–4960.

(68) Saryazdi, S.; Parkin, S.; Grossman, R. B. 1,2-Diamination of Alkenes via 1,3-Dipolar Cycloaddition with Azidium Ions or Azides. *Org. Lett.* **2023**, *25* (2), 331–335.

(69) Liu, F.; Gou, S.; Chen, F.; Fang, L.; Zhao, J. Study on Antitumor Platinum(II) Complexes of Chiral Diamines with Dicyclic Species as Steric Hindrance. *J. Med. Chem.* **2015**, *58* (16), 6368–6377.

(70) Lorenzo, J.; Delgado, A.; Montaña, Á. M.; Mesas, J. M.; Alegre, M.-T.; Rodríguez, M. d. C.; Avilés, F.-X. Synthesis, biological evaluation and SAR studies of novel bicyclic antitumor platinum(IV) complexes. *Eur. J. Med. Chem.* **2014**, *83*, 374–388.

(71) Dai, Z.; Wang, Z. Photoactivatable Platinum-Based Anticancer Drugs: Mode of Photoactivation and Mechanism of Action. *Molecules* **2020**, *25*, 5167.

(72) Biagini, M. C.; Ferrari, M.; Lanfranchi, M.; Marchiò, L.; Pellinghelli, M. A. Chirality in mononuclear square planar complexes. *J. Chem. Soc., Dalton Trans.* **1999**, No. 10, 1575–1580.

(73) Grygorenko, O. O.; Radchenko, D. S.; Volochnyuk, D. M.; Tolmachev, A. A.; Komarov, I. V. Bicyclic Conformationally Restricted Diamines. *Chem. Rev.* **2011**, *111* (9), 5506–5568.

(74) Shechter, H.; Gardikes, J. J.; Cantrell, T. S.; Tiers, G. V. D. Products and stereochemistry of reactions of dinitrogen tetroxide with. DELTA.9,10-octalin, norbornene, cyclooctatetraene, 6,6-diphenylfulvene, and indene. *J. Am. Chem. Soc.* **1967**, *89* (12), 3005–3014.

(75) Ghosh, A. K.; Sarkar, A.; Brindisi, M. The Curtius rearrangement: mechanistic insight and recent applications in natural product syntheses. *Org. Biomol. Chem.* **2018**, *16* (12), 2006–2027.

(76) Norsikian, S.; Beretta, M.; Cannillo, A.; Martin, A.; Retailleau, P.; Beau, J.-M. Synthesis of enantioenriched 1,2-trans-diamines using the borono-Mannich reaction with N-protected α -amino aldehydes. *Chem. Commun.* **2015**, *51* (49), 9991–9994.

(77) Norsikian, S.; Beretta, M.; Cannillo, A.; Auvray, M.; Martin, A.; Retailleau, P.; Iorga, B. I.; Beau, J.-M. Stereoselective Synthesis of 1,2-trans-Diamines Using the Three-Component Borono-Mannich Condensation – Reaction Scope and Mechanistic Insights. *Eur. J. Org. Chem.* **2017**, *2017* (14), 1940–1951.

(78) Tang, M.-C.; Tsang, D. P.-K.; Wong, Y.-C.; Chan, M.-Y.; Wong, K. M.-C.; Yam, V. W.-W. Bipolar Gold(III) Complexes for Solution-Processable Organic Light-Emitting Devices with a Small Efficiency Roll-Off. *J. Am. Chem. Soc.* **2014**, *136* (51), 17861–17868.

(79) Kung, K. K.-Y.; Ko, H.-M.; Cui, J.-F.; Chong, H.-C.; Leung, Y.-C.; Wong, M.-K. Cyclometalated gold(III) complexes for chemoselective cysteine modification via ligand controlled C–S bond-forming reductive elimination. *Chem. Commun.* **2014**, *50* (80), 11899–11902.

(80) Ko, H.-M.; Kung, K. K.-Y.; Cui, J.-F.; Wong, M.-K. Bis-cyclometalated gold(III) complexes as efficient catalysts for synthesis of propargylamines and alkylated indoles. *Chem. Commun.* **2013**, *49* (78), 8869–8871.

(81) Sinha, N.; Wenger, O. S. Photoactive Metal-to-Ligand Charge Transfer Excited States in 3d6 Complexes with Cr0, MnI, FeII, and CoIII. *J. Am. Chem. Soc.* **2023**, *145* (9), 4903–4920.

(82) Li, L.; Bai, F.; Zhang, H.; Li, H. DFT/TDDFT investigation on bis-cyclometalated alkynylgold(III) complex: Comparison of absorption and emission properties. *Sci. China Chem.* **2013**, *56* (5), 641–647.

(83) Yang, B.; Zhang, Q.; Zhong, J.; Huang, S.; Zhang, H. X. Ab initio and DFT study of luminescent cyclometalated N-heterocyclic carbene organogold(III) complexes. *J. Mol. Model.* **2012**, *18* (6), 2543–2551.

(84) Kuo, H.-H.; Kumar, S.; Omongos, R. L.; T. do Casal, M.; Usteri, M. E.; Wörle, M.; Escudero, D.; Shih, C.-J. Design and Synthesis of Asymmetric Au(III) Complexes Exhibiting Bright Anisotropic Emission for High-Performance Organic Light-Emitting Diodes. *Advanced Optical Materials* **2023**, *11* (12), 2202519.

(85) Schmidt, C.; Zollo, M.; Bonsignore, R.; Casini, A.; Hacker, S. M. Competitive profiling of ligandable cysteines in *Staphylococcus aureus* with an organogold compound. *Chem. Commun.* **2022**, *58* (36), 5526–5529.

(86) Thomas, S. R.; Bonsignore, R.; Sánchez Escudero, J.; Meier-Menches, S. M.; Brown, C. M.; Wolf, M. O.; Barone, G.; Luk, L. Y. P.; Casini, A. Exploring the Chemoselectivity towards Cysteine Arylation by Cyclometallated AuIII Compounds: New Mechanistic Insights. *ChemBioChem.* **2020**, *21* (21), 3071–3076.

(87) Wenzel, M. N.; Bonsignore, R.; Thomas, S. R.; Bourissou, D.; Barone, G.; Casini, A. Cyclometalated AuIII Complexes for Cysteine Arylation in Zinc Finger Protein Domains: towards Controlled Reductive Elimination. *Chem. Eur. J.* **2019**, *25* (32), 7628–7634.

(88) de Paiva, R. E. F.; Du, Z.; Nakahata, D. H.; Lima, F. A.; Corbi, P. P.; Farrell, N. P. Gold-Catalyzed C–S Aryl-Group Transfer in Zinc Finger Proteins. *Angew. Chem., Int. Ed.* **2018**, *57* (30), 9305–9309.

(89) Kim, J. H.; Mertens, R. T.; Agarwal, A.; Parkin, S.; Berger, G.; Awuah, S. G. Direct intramolecular carbon(sp₂)–nitrogen(sp₂) reductive elimination from gold(III). *Dalton Trans.* **2019**, *48* (18), 6273–6282.

(90) Olelewe, C.; Kim, J. H.; Ofori, S.; Mertens, R. T.; Gukathasan, S.; Awuah, S. G. Gold(III)-P-chirogenic complex induces mitochondrial dysfunction in triple-negative breast cancer. *iScience* **2022**, *25* (5), 104340.

(91) Evans, K. W.; Yuca, E.; Scott, S. S.; Zhao, M.; Paez Arango, N.; Cruz Pico, C. X.; Saridogan, T.; Shariati, M.; Class, C. A.; Bristow, C. A.; Vellano, C. P.; Zheng, X.; Gonzalez-Angulo, A. M.; Su, X.; Tapia, C.; Chen, K.; Alkanat, A.; Lim, B.; Tripathy, D.; Yap, T. A.; Francesco, M. E. D.; Draetta, G. F.; Jones, P.; Heffernan, T. P.; Marszalek, J. R.; Meric-Bernstam, F. Oxidative Phosphorylation Is a Metabolic Vulnerability in Chemotherapy-Resistant Triple-Negative Breast Cancer. *Cancer Res.* **2021**, *81* (21), 5572–5581.

(92) McDonnell, M. A.; Wang, D.; Khan, S. M.; Vander Heiden, M. G.; Kelekar, A. Caspase-9 is activated in a cytochrome c-independent manner early during TNF α -induced apoptosis in murine cells. *Cell Death Differ.* **2003**, *10* (9), 1005–1015.

(93) Perillo, B.; Di Donato, M.; Pezone, A.; Di Zazzo, E.; Giovannelli, P.; Galasso, G.; Castoria, G.; Migliaccio, A. ROS in cancer therapy: the bright side of the moon. *Exp. Mol. Med.* **2020**, *S2* (2), 192–203.

(94) Olelewe, C.; Awuah, S. G. Mitochondria as a target of third row transition metal-based anticancer complexes. *Curr. Opin. Chem. Biol.* **2023**, *72*, 102235.

(95) Yetkin-Arik, B.; Vogels, I. M. C.; Nowak-Sliwinska, P.; Weiss, A.; Houtkooper, R. H.; Van Noorden, C. J. F.; Klaassen, I.; Schlingemann, R. O. The role of glycolysis and mitochondrial respiration in the formation and functioning of endothelial tip cells during angiogenesis. *Sci. Rep.* **2019**, *9* (1), 12608.

(96) Gu, X.; Ma, Y.; Liu, Y.; Wan, Q. Measurement of mitochondrial respiration in adherent cells by Seahorse XF96 Cell Mito Stress Test. *STAR Protoc.* **2021**, *2* (1), 100245.

(97) Hill, B. G.; Benavides, G. A.; Lancaster, J. R., Jr.; Ballinger, S.; Dell’Italia, L.; Zhang, J.; Darley-Usmar, V. M. Integration of cellular bioenergetics with mitochondrial quality control and autophagy. *Biol. Chem.* **2012**, *393* (12), 1485–1512.

(98) Hill, B. G.; Dranka, B. P.; Zou, L.; Chatham, J. C.; Darley-Usmar, V. M. Importance of the bioenergetic reserve capacity in response to cardiomyocyte stress induced by 4-hydroxynonenal. *Biochem. J.* **2009**, *424* (1), 99–107.

(99) Marchetti, P.; Fovez, Q.; Germain, N.; Khamari, R.; Kluza, J. Mitochondrial spare respiratory capacity: Mechanisms, regulation, and significance in non-transformed and cancer cells. *FASEB J.* **2020**, *34* (10), 13106–13124.